COO-1112-191

ELECTRO-PRIMAKOFF EFFECT

D. N. Goswami*

National Research Council of Canada

Ottawa, Ontario K1A OR6, Canada

and

N. Horwitz

Physics Department, Syracuse University,

Syracuse, New York 13210

and

D. P. Majumdar

Harrison M. Randall Laboratory of Physics

The University of Michigan, Ann Arbor, Michigan 48104

*NRCC Postdoctoral Fellow 1971-1973.

NRCC Publication no. 13017

DISCLAIMER

ABSTRACT

We discuss the electro-Primakoff process (e + Nucleus)→ (e + Nucleus + π°) where an off-mass-shell photon interacts with the Coulomb field of the nucleus to produce a π° meson. Unlike the Dalitz pair decay of the π°, e.g., $\pi^\circ \to e^+e^-\gamma$, here the exchanged photon can have a comparitively large four-momentum square ($|k^2|$) and can be controlled by the electron energy and the scattering angle. This process can thus be a direct means for measuring the momentum dependence of the $\pi^\circ \to \gamma\gamma$ coupling when the photons are off-mass-shell. We have plotted the differential electro-Primakoff cross-section for different values of k^2 for the case when the momentum dependence of the $\pi^\circ\gamma\gamma$ coupling is neglected, i.e., we have used the value for the coupling constant obtained from the $\pi^\circ \to \gamma\gamma$ decay. We have considered two representative target materials corresponding roughly to hydrogen and lead. The dependence of the cross-section on the angles made by the outgoing pion ($\theta_{\gamma\pi}$, and $\phi_{\gamma\pi}$) and on the electromagnetic form factor is also discussed in some detail. The electro-Primakoff peak occurs at an angle $\theta_E = (|k^2| + m_\pi{}^2)/2E_\pi{}^2$ with respect to the virtual photon direction and the cross-section has a unique $\phi_{\gamma\pi}$ dependence of the form $C_1(C_2 + \mathrm{Sin}^2\phi_{\gamma\pi})$. Finally, the contribution of the background processes are discussed. Important among these are coherent electro-nuclear and bremsstrahlung production of π° mesons. We have estimated the coherent background by using the Weizsäcker-Williams approximation procedure

and found its contribution at the position of the electro-Primakoff peak to be small so long as $|k^2|/E_\pi^2$ is small. The main bremsstrahlung π° peak (Primakoff peak) would be in the very forward direction and would not interfere with the electro-Primakoff peak. Also the coherent bremsstrahlung background contribution can be resolved by a suitable choice of the kinematics.

I. INTRODUCTION

The production of π^0 mesons in the Coulomb field of a nucleus, originally suggested by Primakoff[1], has been studied extensively during the past ten years[2-8]. This has furnished information on the two-photon coupling constant of the pion when one of the photons is real and the other virtual (space-like). This in turn produces the lifetime of the π^0 meson. The object of this paper is to investigate the electro-Primakoff effect; that is, we shall discuss the possibility of performing $\pi^0(\eta)$-production experiments with electron beams and study the observations to be expected. In this case we note that both the photons are space-like and hence this will give us more insight into the nature of the off-shell two photon-pion coupling. Our calculations will also give some estimates of the Coulomb production background for the inelastic lepton-nucleon scattering experiments. This is important to know in the present context of the inelastic experiments being planned at higher and higher energies. Furthermore, since in this electro-production process we can calculate exactly the matrix element, it would also be interesting to see how good the Weizsäcker-Williams approximation, which was invented to obtain results for fast moving particles, work in practice. From an experimental point of view this will have some advantages over the Primakoff effect in

the sense that it is possible to measure accurately both the incoming and outgoing momentum and energy of the electron, and hence it would enable us to understand the space-like character of the photon in more detail. Our final comment is that this experiment should be performed at least to confirm and increase our understanding of the production processes via Coulomb interactions.

The plan of the paper is as follows. In Section II we discuss the kinematics and derive formulas necessary for the evaluation of the cross-section. We note in advance that in this case, since we have two outgoing particles, we shall have an extra azimuthal angle to measure between the outgoing electron and the pion planes. This may be an interesting aspect of investigation for the electro-Primakoff effect. We shall also derive here expressions for the electro-Primakoff effect in terms of the photo-Primakoff effect in the Weizsäcker-Williams approximation. In Section III we shall make some small angle approximations and discuss the experimental feasibility of the electro-Primakoff process. We present graphs showing the behaviour of the cross-section as a function of the observed variables in section IV. We also discuss there the effect of the nuclear form factor on the cross-section. In section V the general background processes, which can affect this experiment will be studied. Notable of these is the electro-nuclear production of the π° mesons. This part of the analysis will be similar to that

of the photo-Primakoff effect. However, we have to estimate these electro-results from the corresponding photo-results using some approximation procedure since the data for electro-production of π^o meson is not presently available. We shall also make some comments on the Bremsstrahlung effect.

II. KINEMATICS AND CROSS-SECTION CALCULATION

The kinematics and the notation for the electro-Primakoff effect are shown in Fig. 1, which represents the process

$$e(p_i) + \text{Nucleus} \longrightarrow e(p_f) + \text{Nucleus} + \pi^o(p_\pi)$$

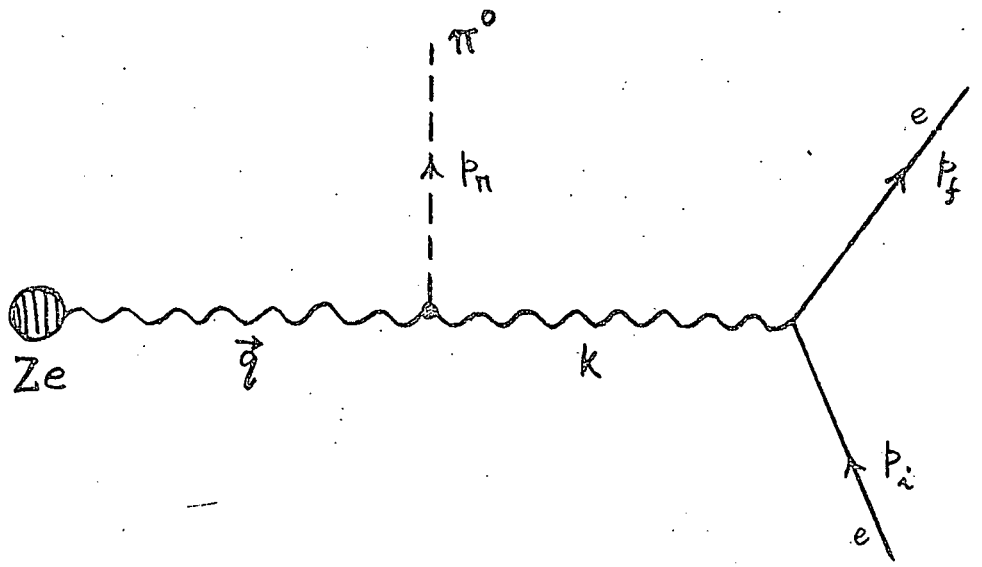

FIGURE I.

p_i and p_f are the initial and final momenta of the electrons, k is the momentum transfer to the photon from the electrons, $q = (0,\vec{q})$ is the momentum of the Coulomb photon and p_π is the momentum of the neutral pion produced. k^2 and q^2 are both space-like, i.e. negative in our metric, and $p_\pi^2 = m_\pi^2$. Ze is the total charge of the nucleus, our Coulomb source.

First let us recapitulate the Primakoff-effect, where $k^2 = 0$. Let the real two photon decay of the π° meson be described by a Lagrangian

$$L(x) = \frac{1}{8} \lambda \, \varepsilon_{\mu\nu\rho\delta} \, F^{\mu\nu}(x) \, F^{\rho\delta}(x) \, \phi_\pi(x), \qquad (1)$$

where ϕ_π and $F_{\mu\nu} = \partial_\mu A_\nu - \partial_\nu A_\mu$ represent the π° and the photon fields respectively, and $\varepsilon_{\mu\nu\rho\delta}$ is the totally anti-symmetric tensor. To conform with the usual notations in terms of the electric and magnetic fields E and H, we note that L(x) can also be written as

$$L(x) = \lambda E.H \, \phi_\pi(x) \qquad (2)$$

The lifetime of the π° meson is then given in terms of the coupling constant λ :

$$\tau_\pi^{-1} = \Gamma_{\pi^\circ \to 2\gamma} = \frac{1}{64\pi} \lambda^2 m_\pi^3 \qquad (3)$$

For the Coulomb case, we have[9]

$$A^\mu(\vec{q}) = \frac{Ze}{|\vec{q}|^2} \, 2\pi \, \delta(E_\pi - E_\gamma) g^{\mu o} \qquad (4)$$

Suppose that the π°-2γ coupling constant when one photon is real and the other virtual is same as the coupling constant of the π° meson decaying into two real photons. This is not a bad approximation since the squared four momentum of the virtual photon is very small in the kinematic region which is important for the Primekoff process. The Primekoff cross-section for an unpolarized photon beam can then be easily calculated from eqs. (1) and (4) in terms of the pion lifetime.

$$\frac{d\sigma^P}{d\Omega_\pi} = \frac{8Z^2\alpha}{m_\pi^3\tau_\pi} \left|F_{e.m.}(\vec{q}^2)\right|^2 \frac{p_\pi^3 E_\pi}{\vec{q}^4} \sin^2\theta_{\gamma\pi}, \qquad (5)$$

where $\alpha = 1/137$, $\theta_{\gamma\pi}$ is the angle made by the π° momentum $\vec{p}_\pi$ with the incoming photon momentum $\vec{k}$, and $F_{e.m.}(q^2)$ is the nuclear electromagnetic form factor, corrected for absorption of the outgoing pion[3,4].

The phenomenological π°-2γ vertex is, strictly speaking, a function of the two photon momenta. Let us denote this by $\lambda(q^2, k^2)$. Since for the Primekoff process the incoming photon is real ($k^2 = 0$), and $|q^2| = \vec{q}^2 = m_\pi^4/2E_\pi^2 < 0.01\ (\text{Gev/c})^2$ at the forward peak of the cross-section, we can neglect the momentum dependence of the coupling constant λ, i.e. $\lambda(q^2,0) = \lambda(0,0) = \lambda$.

However, for the electro-Primakoff effect k^2 can be quite large and, therefore, a study of this process should

reveal the momentum dependence, if any, of the π^o-2γ coupling constant.

The calculation of the cross-section for the electro-Primakoff effect is straightforward and can be expressed as

$$\frac{d^3\sigma^{EP}}{dE_f d\Omega_f d\Omega_\pi} = \frac{\lambda^2(q^2,k^2)}{8\pi^3 v_i} \alpha^2 Z^2 |\vec{p}_\pi| \, (E_f/E_i) k^{-4} (\vec{q})^{-4}$$
$$\times \left[2(\vec{p}_i \vec{r})(\vec{p}_f . \vec{r}) + \frac{1}{2} r^2 k^2\right] \left|F_{e.m.}(\vec{q}^2)\right|^2, \quad (6)$$

where we have defined a new space-like vector

$$r = (0, \vec{k} x \vec{p}_\pi) \quad (7)$$

v_i is the velocity of the incoming electron and E_i and E_f are the energies of the initial and final electrons respectively. A comparison with the photo-effect immediately tells us that electro-Primakoff effect will be important only when α/k^2 is not too small, and consequently the scattering angle of the electron, θ_e, should be small.

For the electro-Primakoff effect it is convenient to define the angle made by the outgoing pion momentum with respect to the virtual photon momentum. This is also the angle measured in the Primakoff effect. The co-ordinate system that we shall employ here is shown in fig. 2. The Z-axis is taken along the photon momentum $\vec{k}$ and the X-axis is in the plane defined by $\vec{p}_i$, $\vec{p}_f$ and $\vec{k}$ vectors. The direction of $\vec{p}_\pi$

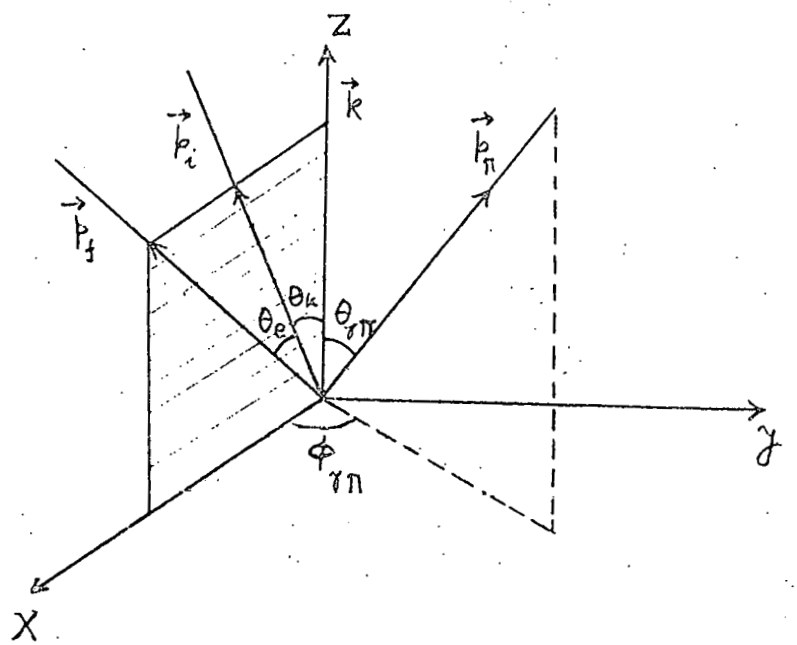

is defined by the angles $\theta_{\gamma\pi}$ and $\phi_{\gamma\pi}$ as shown in fig. 2. We shall approximate $|\vec{p}_i|, |\vec{p}_f|$ by E_i and E_f whenever appropriate. Then we obtain

$$(\vec{p}_i,\vec{r})(\vec{p}_f,\vec{r}) = E_i^2 E_f^2 \vec{p}_\pi^2 \mathrm{Sin}^2\theta_{\gamma\pi} \mathrm{Sin}^2\theta_{\gamma\pi} \mathrm{Sin}^2\theta_e \tag{8}$$

$$r^2 = -\vec{r}^2 = -(E_\pi^2 - k^2)\vec{p}_\rho^2 \, \mathrm{Sin}^2\theta_{\gamma\pi} \tag{9}$$

$$\vec{q}^2 = 2E_n^2 - k^2 - m^2 - 2|\vec{p}| \, (E_\pi^2 - m_\pi^2)^{1/2} \mathrm{Cos}\theta_{\gamma\pi} \tag{10}$$

$$\text{and} \quad k^2 = 2m_e^2 - 2E_i E_f + 2|\vec{p}_i||\vec{p}_f| \mathrm{Cos}\ \theta_e \tag{11}$$

Eq. (6) supplemented with eqs. (8) to (11), which expresses all the variables in terms of measurable quantities, is our basic expression for the electro-Primakoff effect.

For later use we shall now employ the Weizäcker-Williams[10] approximation procedure to write down the result for the electro-production process in terms of the photo-production process. We remind the reader that this is a useful technique for obtaining leading high energy behaviour of electro-production cross-section only if the electron is scattered into a small forward angle. Further it is to be understood that this approximation[11] will be correct only when the azimuthal angle of the electron is integrated over. We then find (see Appendix A for derivation and discussion) that

$$\left[\frac{d^3\sigma}{dE_f d\Omega_f d\Omega_\pi}\right]_{\text{electro-}} = \frac{\alpha}{2\pi^2}\ \frac{E_f E_\pi}{E_i \nu_i}\ \frac{1}{k^4}\ \left[-k^2 + \frac{2E_i^2 E_f^2}{\vec{k}^2}\ \text{Sin}^2\theta_e + \ldots\ldots\right] \times \left[\frac{d\sigma}{d\Omega_\pi}\right]_{\text{photo-}} \qquad (12)$$

III. SMALL ANGLE APPROXIMATION AND COMPARISON WITH PRIMAKOFF EFFECT

For the Primakoff effect, when $\theta_{\gamma\pi}$ is small we can write

$$\vec{q}^2 \simeq E_\pi^2\ \left(\theta_{\gamma\pi}^2 + \frac{m_\pi^4}{4E_\pi^4}\right) \qquad (13)$$

and hence we have from eq. (5)

$$\Delta\sigma^p = \left(\frac{d\sigma^p}{d\Omega_\pi}\right)\Delta\Omega_{\pi-} = \frac{8Z^2\alpha}{m_\pi^3 \tau_\pi}\ \frac{\theta_{\gamma\pi}^2}{(\theta_{\gamma\pi}^2 + \theta_p^2)}\ \left|F_{e.m}(\vec{q}^2)\right|^2 \Delta\Omega_\pi \qquad (14)$$

where we have defined

$$\theta_p = \frac{1}{2}\left(\frac{m_\pi}{E_\pi}\right)^2 \qquad (15)$$

Thus for the Primakoff effect, the cross-section is peaked at an angle $\theta_{\gamma\pi} = \theta_p$ near the forward direction. This enables Primakoff effect to be distinguished from the background processes.

For a similar analysis of the electro-Primakoff effect, it is convenient to rewrite the cross-section in terms of the five independent variables E_i, E_f, θ_e, $\theta_{\gamma\pi}$, and $\phi_{\gamma\pi}$. As mentioned earlier θ_e must be small; we then obtain

$$k^2 \simeq -[(m_e E_\pi/E)^2 + (E\theta_e)^2] \qquad (16)$$

where we have defined $E^2 = E_i E_f$ and have neglected terms of order $\theta_e^2 m_e^2$, m_e^4/E^2 and $\theta_e^4 E^2$ which are indeed small. As in the Primakoff effect we also expect here a peaking behaviour of the cross section in the forward direction. For small $\theta_{\gamma\pi}$ we can write

$$2(\vec{p}_i.\vec{r})(\vec{p}_f.\vec{r}) + \frac{1}{2}r^2k^2 \simeq \vec{p}_\pi^{\,2}\theta^2_{\gamma\pi}[2E^4\theta_e^2\sin^2\phi_{\gamma\pi} + \frac{1}{2}(E_\pi^2 + E^2\theta_e^2)(m_e^2E_\pi^2/E^2 + E^2\theta_e^2)] \qquad (17)$$

We further find that when $E_\pi^2 >> -k^2$ and $E_\pi^2 >> m_\pi^2$,

$$\vec{q}^{\,2} \simeq E_\pi^2(\theta^2_{\gamma\pi} + \theta_E^2) \qquad (18)$$

where

$$\theta_E = \frac{-k^2 + m_\pi^2}{2E_\pi^2} \qquad (19)$$

Using (17) and (18) in (6) we obtain

$$\frac{d^3\sigma^{EP}}{dE_f d\Omega_f d\Omega_\pi} = \frac{|\lambda(q^2,k^2)|^2}{8\pi^3 v_i}\alpha^2 Z^2 \frac{|\vec{p}_\pi|^3 E_f}{E_\pi^4 E_i} k^{-4} \frac{\theta_{\gamma\pi}^2}{(\theta_{\gamma\pi}^2+\theta_E^2)^2} |F_{e.m}(\vec{q}^2)|^2$$

$$\times [2E^4\theta_e^2 \sin^2\phi_{\gamma\pi} + \tfrac{1}{2}(E_\pi^2 + E^2\theta_e^2)(m_e^2E_\pi^2/E^2 + E^2\theta_e^2)] \qquad (20)$$

Thus the electro-Primakoff differential cross-section would peak at an angle $\theta_{\gamma\pi}\simeq\theta_E$. Since k^2 is negative, comparing (15) and (19) we note that the 'peak' angle θ_E is greater than the corresponding angle θ_p for the Primakoff process.

If $-k^2 \simeq E_\pi^2 >> m_\pi^2$, we obtain $\vec{q}^2 \simeq \sqrt{2}\, E_\pi|\vec{p}_\pi|(\theta_{\gamma\pi}^2 + \theta_{E'}^2)$

where

$$\theta_{E'} \simeq \frac{\sqrt{2}\, E_\pi - |\vec{p}_\pi|}{(\sqrt{2}\, E_\pi|\vec{p}_\pi|)^{1/2}} > \frac{\sqrt{2}-1}{2^{1/4}} \simeq .35 \qquad (21)$$

In this case the electro-Primakoff peak would be very broad and would occur at a region where the dominant contribution to the π° production cross-section would come from the background processes. Hence we would restrict ourselves to the case $E_\pi^2 >> -k^2$.

To obtain some numerical estimates of the electro-Primakoff cross-section let us assume that we can approximate $\lambda(q^2,k^2)$ by the π° decay coupling constant. With the small angle approximation written above, and assuming a

similar kinematic region, we can relate the electro-Primakoff process to the photo-Primakoff process in a simple way. We shall also assume here that the nuclear form factor effect is same for both the processes. Let us write

$$\Delta\sigma^{EP} = \frac{d^3\sigma^{EP}}{dE_f d\Omega_f d\Omega_\pi} \Delta E_f \ \Delta\Omega_f \Delta\Omega_\pi \tag{22}$$

We discuss separately two cases depending on the value of θ_e compared with $m_e E_\pi/(E_i E_f)$.

Case 1. $\theta_e < \frac{m_e E_\pi}{E_i E_f}$

In this case $-k^2 \simeq m_e^2(E_\pi^2/E^2) << E_\pi^2$. Then comparing (20) with (14) we get

$$\Delta\sigma^{EP} \simeq \frac{\alpha}{2\pi^2 v_i} \frac{E_f^2}{m_e^2} \left(\frac{\theta_{\gamma\pi}^2 + \theta_P^2}{\theta_{\gamma\pi}^2 + \theta_E^2} \right)^2 \Delta\sigma^P \left(\frac{\Delta E_f}{E_\pi} \right) \Delta\Omega_f \tag{23}$$

Case 2. $\theta_e > \frac{m_e E_\pi}{E_i E_f}$

In this case k^2 could be large. However, for reasons discussed already (see after eq. (21)), we would restrict ourselves to $E_\pi^2 >> -k^2$.

We then obtain

$$\Delta\sigma^{EP} \simeq \frac{\alpha}{\pi^2 v_i} \frac{E_f}{E_i} \left(\frac{\theta_{\gamma\pi}^2 + \theta_p^2}{\theta_{\gamma\pi}^2 + \theta_E^2} \right)^2 \frac{2E^2 \sin^2\phi_{\gamma\pi} + \frac{1}{2} E_\pi^2}{E^2\theta_e^2}$$

$$\times \Delta\sigma^P . (\Delta E_f/E_\pi) \Delta\Omega_f \tag{24}$$

To obtain a rough estimate of the cross-section let us assume that $E_i \sim E_f \sim E \sim E_\pi$, and $\Delta E_f/E_\pi \simeq 1/5$. For very small electron scattering angle (Case 1), we take $o < \theta_e E \leqslant m_e$. Let us further assume that $\theta_E \simeq \theta_p$, and replace $\Delta\Omega_f$ by $2\pi\theta_e^2 = 2\pi(m_e/E)^2$

Then from (23) we obtain

$$\Delta\sigma^{EP} \sim 4 \times 10^{-4}\ \Delta\sigma^{P} \tag{25a}$$

We next consider the case $\theta_e > m_e E_\pi/E_i E_f$. We shall take $m_e/E < \theta_e < m_\pi/E$, and assume that $(\theta_{\gamma\pi}^2 + \theta_P^2)^2/(\theta_{\gamma\pi}^2 + \theta_E^2)^2 \sim 1/4$. We further take $\langle \mathrm{Sin}^2\phi_\gamma \rangle = \frac{1}{2}$, $\Delta\Omega_e = 2\pi\theta_e d\theta_e$, and integrate (24) over θ_e for m_e/E to m_π/E. This gives

$$\Delta\sigma^{EP} \sim 10^{-3}\ \Delta\sigma^{P} \tag{25b}$$

For Primakoff effect $Z^{-2}\Delta\sigma^P$ is of the order of 10^{-4} micro-barn (we assumed $\Delta\Omega_\pi \simeq 2\pi\theta_P^2$), so that $\Delta\sigma^{EP} \sim 10^{-8}$ μb. A more exact evaluation of the electro-Primakoff cross-section (eq.(28)) for E_i = 10 Gev, and E_f = 8 Gev and 4 Gev, as a function of k^2 is shown in Fig. 5. These estimates show that with a reasonable incident electron flux (say, of the order of 10^{11} electrons/sec.) and moderately good detection efficiency (∼0.1) the electro-Primakoff effect should be within the range of experimental measurement.

IV. ELECTRO-PRIMAKOFF CROSS-SECTION

In this section we shall study the behaviour of the electro-Primakoff cross-section as a function of the different observed variables and shall make numerical estimates. If we keep the initial and final energies of the electron fixed we have only three variables left, namely, the pion production angle $\theta_{\gamma\pi}$, the azimuthal angle $\phi_{\gamma\pi}$ and the electron scattering angle θ_e (which essentially defines k^2). In the following we shall keep the initial electron energy fixed and consider two values for the final electron energy. The kinematic region that we shall be interested in is $E_\pi \sim$ Gev , and $E_\pi^2 >> -k^2$. We shall also discuss here the dependence of the cross-section on the nuclear form factor.

(i) $\phi_{\gamma\pi}$ dependence: Since we have two outgoing particles (the electron and the pion), we can measure the azimuthal angular dependence of the outgoing pion with respect to the electron scattering plane. Here we have a unique prediction for the $\phi_{\gamma\pi}$ dependence of the cross-section, namely,

$$\frac{d\sigma^{EP}}{d\phi_{\gamma\pi}} = f_1(E_i, E_f, \theta_e, \theta_{\gamma\pi})[\mathrm{Sin}^2\phi_{\gamma\pi} + f_2(E_i, E_f, \theta_e)] ,$$

where f_1 and f_2 are functions independent of $\phi_{\gamma\pi}$; for $\theta_e >> m_e(E_i - E_f)/E_iE_f$, f_2 is given by

$$f_2(E_i, E_f, \theta_e) \simeq \frac{(E_i - E_f)^2}{4E_iE_f}$$

If we take $E_f > E_i/2$, then $f_2 < 0.13$. Thus if we set $\theta_{\gamma\pi}$ at the peak ($\theta_{\gamma\pi} \simeq \theta_E$), and $E_f \gtrsim E_i/2$, it should be quite easy to to observe the $Sin^2\phi_{\gamma\pi}$ dependence of the electro-Primakoff cross-section

(ii) $\theta_{\gamma\pi}$ dependence: we observe that the $\theta_{\gamma\pi}$ dependence of the electro-Primakoff cross-section comes only from the factors $[2(\vec{p}_i.\vec{r})(\vec{p}_f.\vec{r}) + \frac{1}{2} r^2k^2]$ and $\vec{q}^2$. Hence, if we consider the cross-section divided by $|F_{e.m.}(\vec{q}^2)|^2$ the $\theta_{\gamma\pi}$ dependence for small $\theta_{\gamma\pi}$ will always be of the type

$$Z^{-2}|F_{e.m.}(\vec{q}^2)|^{-2} \frac{d\sigma^{EP}}{d\Omega_\pi} \propto \frac{\theta^2_{\gamma\pi}}{(\theta^2_{\gamma\pi} + \theta^2_E)^2} \qquad (28)$$

where θ_E depends only on k^2 and E_π^2 as given in eq. (19). If we take $|F(\vec{q}^2)|^2 = 1.0$, i.e., neglect the electromagnetic form-factor effect, the peaking behaviour of $Z^{-2} \frac{d\sigma^{EP}}{d\Omega_\pi}$ will be the same for all targets. This is shown in Fig. 3, where we have plotted $Z^{-2} \frac{d\sigma^{EP}}{d(Cos\theta_{\gamma\pi})}$ as a function of $\theta_{\gamma\pi}/\theta_E$.

(iii) Form factor dependence (k^2 fixed): Earlier, in discussing the $\theta_{\gamma\pi}$ dependence of the differential cross-section we assumed $F_{e.m.}(\vec{q}^2) = 1$. This gave us a universal curve for $Z^{-2} \frac{d\sigma^{EP}}{d\Omega_\pi}$ for all targets. This is no longer true when the form factor effect is taken into account. The effect of the form

factor on the cross-section is shown in Fig. 4, where we have plotted

$$Z^{-2}\frac{d\sigma^{EP}}{d(\cos\theta_{\gamma\pi})} = Z^{-2}\int_0^{2\pi} d\phi_{\gamma\pi}\int_{0.95<k^2>}^{1.05<k^2>} dk^2 \int_{0.95<E_f>}^{1.05<E_f>} dE_f \frac{d^3\sigma^{EP}}{dE_f dk^2 d\Omega_{\gamma\pi}} \quad (29)$$

as a function of $\theta_{\gamma\pi}/\theta_E$ for E_i = 10 Gev and $|k^2|$ = 0.5 $(Gev/c)^2$. Fig. 4a shows the case for E_f = 4 Gev and Fig. 4b shows that for E_f = 8 Gev. Since the electromagnetic form factor falls off exponentially with increase in $\vec{q}^2$, which depends on $\theta_{\gamma\pi}$ (see Eq. (18)), the form factor effect causes the position of the electro-Primakoff peak to shift from $\theta_{\gamma\pi} = \theta_E$ towards a smaller angle. For large b (heavy targets) and $|k^2|/E_\pi^2$ large (>0.1) the shift can be appreciable. This is shown in fig. 6.

(iv) k^2 dependence: We note that in the kinematic region of our interest the momentum transfer to the target nucleus is given by $\vec{q}^2 \simeq E_\pi^2\theta_{\gamma\pi}^2 + (m_\pi^2 - k^2)^2/4E_\pi^2$. Now, if the momentum dependence of the electromagnetic form factor is included, the cross-section will fall off faster with increase in $|k^2|$. The exact expression for the form factor is not known. Here we shall parametrize it in the form

$$|F_{e.m.}(\vec{q}^2)|^2 = e^{-b\vec{q}^2} \quad (30)$$

and consider values of b = 0, 10, and 300 $(Gev/c)^{-2}$. The value b = 0 corresponds to neglecting the momentum dependence of the

form factor, while b = 10 $(Gev/c)^{-2}$, and 300 $(Gev/c)^{-2}$ correspond roughly to the cases for hydrogen and lead targets respectively. The dependence of the electro-Primakoff cross-section on $|k^2|$ for the three values of b is shown in Fig. 5. The cross-section that we have plotted is obtained by integrating the differential cross-section given by eq. (20) (scaled by a factor of Z^{-2}) over E_f, k^2, $\theta_{\gamma\pi}$, and $\phi_{\gamma\pi}$ in the range $0.95 <E_f> \leq E_f \leq 1.05 <E_f>$, $0.95 <|k^2|> \leq |k^2| \leq 1.05 <|k^2|>$, $0 \leq \theta_{\gamma\pi} \leq 2.5\ \theta_E$ and $0 \leq \phi_{\gamma\pi} \leq 2\pi$ respectively, i.e., we have plotted

$$Z^{-2}\Delta\sigma^{EP} = Z^{-2} \int_{0.95<E_f>}^{1.05<E_f>} dE_f \int_{0.95<k^2>}^{1.05<k^2>} dk^2 \int_0^{2\pi} d\phi_{\gamma\pi} \int_0^{2.5\theta_E} d\theta_{\gamma\pi} \frac{d^3\sigma^{EP}}{dE_f dk^2 d\Omega_\pi} \qquad (31)$$

against $<|k^2|>$. Note that the nuclear form factor effect becomes very important for heavy target materials as $|k^2|$ increases.

The $\pi^\circ\gamma\gamma$ coupling constant is usually parameterized for small k^2, i.e., $k^2 < m_\pi^2$, by

$$\lambda(k^2,0) = \lambda(0,0) \left[1 + a\ (k^2/m_\pi^2) + O((k^2/m_\pi^2)^2) \right]$$

The theoretical values predicted for the parameter 'a' are small and positive[12], while the experimental value obtained from the decay mode $\pi^\circ \to e^+e^-\gamma$ is either negative[13] (bubble chamber experiment) or approximately zero[14] (spark chamber experiment). In our case $|k^2|$ could be quite large and the above parameterization for $\lambda(k^2,0)$ can not be used. For lack of any definitive

knowledge on the momentum dependence of the coupling constant, we have not considered any momentum dependence of the coupling constant $\lambda(k^2,q^2)$ in plotting Figs. 4 and 5, and have used for λ the value obtained from the pion decay rate.

V. Background Processes

The main problems in studying the photo- and electro-Primakoff effects are due to the presence of other important competitive processes. The relative importance of these background processes for the Primakoff effect has been discussed in detail in the literature[2-4]. For the electro-Primakoff effect the complications are essentially the same except for the additional problem of bremsstrahlung radiation followed by photo-emission of the neutral pion. We shall briefly mention here the background problems and shall make some rough estimates of these contributions.

One can classify the background as follows:

(i) Direct nuclear electroproduction of pions by the nucleons inside the nucleus. This can be divided into two parts - coherent cross section roughly proportional to A^2 and incoherent cross section roughly proportional to A, where A is the atomic number of the nucleus. The incoherent contribution is expected to be small compared to the coherent one around the forward direction.

(ii) Neutral pion reabsorption inside the nuclear matter. This can be taken into account by using effective "absorbed form factors" for the nucleus.

(iii) Interference between the electro-Primakoff and electro-nuclear cross-sections.

(iv) Bremsstrahlung radiation producing Primakoff and nuclear pions.

We shall discuss now only the two most important backgrounds, namely the nuclear coherent and the bremsstrahlung production of pions. The cross section for direct electro-production of nuclear π° mesons from target nuclei is not known experimentally. Hence to compare this background with the main process under consideration we have to estimate it by an indirect method. This can be achieved by using the Weizsäcker-Williams approximation procedure applied to the corresponding photo-process. The equation to be used for this purpose is given by Eq. (12). In this approximation one neglects the longitudinal part of the electro-amplitude and suitably approximates the rest near the forward electron scattering angle in terms of the corresponding photo-amplitude. Although crude, this approximation is expected to produce results accurate to within 20% which would be adequate for a rough background estimate. The nuclear coherent cross-section for an incident photon beam can, for our purpose, be represented by

$$\frac{d\sigma^c}{d\Omega_\pi} = C\ A^2\ |\ F_N\ (\vec{q}^2)\ |^2\ \mathrm{Sin}^2\ \theta_{\gamma\pi}\ \ldots \qquad (32)$$

where

A = Atomic weight of the target material,

$\theta_{\gamma\pi}$ = angle between the photon and the outgoing pion momentum,

$F_N(\vec{q}^2)$ = form factor for the nuclear matter distribution in the nucleus corrected for absorption of the outgoing pion,

and $C \sin^2\theta_{\gamma\pi}$ = square of the isospin and spin independent part of the photoproduction amplitude on a single nucleon.

The value of C depends on various factors including the energy of the incident photon beam and the target element. Unfortunately there is no known theory to calculate C; it has to be regarded as a parameter to be determined experimentally. Experimental results[8] have shown that for photon energies 1.5 Gev and 2 Gev, C ranges from about 0.7 to 1.6 mb/Sr for target elements varying from carbon to lead. The form factor $F_N(\vec{q}^2)$ is a complicated function that falls off rapidly with increase in $\vec{q}^2$. If the nucleus is assumed to be a uniform sphere of radius R, where $R = r_o A^{1/3}$, the form factor is given by[4]

$$F_N(\vec{q}^2) = 3\left[\sin|\vec{q}|R - (|\vec{q}|R)\cos|\vec{q}|R\right](|\vec{q}|R)^{-3} \qquad (33)$$

The value of r_o depends on the momentum of the incident particle and the atomic weight of the target; its approximate value is about 1 fermi. For small $\vec{q}$, e.g., $|\vec{q}|R \ll 1$,

$$|F_N(\vec{q}^2)|^2 \simeq 1 - \vec{q}^2R^2/5 \qquad (34)$$

We would like to remark that if we have assumed an exponential form for the form factor, viz., $|F_N(\vec{q}^2)|^2 = e^{-b\vec{q}^2}$, and

identified b with $R^2/5$, so that for small $\vec{q}$ we recover expression (34), we would have obtained b = 6.2(Gev/c)$^{-2}$ for hydrogen and b = 217(Gev/c)$^{-2}$ for lead (we used $R = r_o A^{1/3}$ with r_o = 1.1 fm.). The coherent nuclear production cross-section would be maximum when $|F_N(\vec{q}^2)|^2 \sin^2\theta_{\gamma\pi}$ is maximum. This will occur at an angle

$$\theta_c \simeq \frac{\sqrt{5}}{E_\pi R} \equiv \frac{1}{\sqrt{b}E_\pi} \tag{35}$$

Notice that unlike the electro-Primakoff peaking angle θ_E, θ_c is independent of k^2 but depends only on the target material and the energy of the outgoing pion. In Fig. 7 we have plotted the coherent nuclear production cross-section

$$A^{-2}\frac{d\sigma^c}{d(\cos\theta_{\gamma\pi})} = A^{-2}\int_{00}^{2\pi} d\phi_{\gamma\pi}\int_{0.95<k^2>}^{1.05<k^2>} dk^2 \int_{0.95<E_f>}^{1.05<E_f>} dE_f \frac{d^3\sigma^c}{dE_f dk^2 d\Omega_{\gamma\pi}} \tag{36}$$

as a function of $\theta_{\gamma\pi}/\theta_E$ for different values of $|k^2|$ and E_π, and for targets of hydrogen and lead (dashed curves). In evaluating the R.H.S. of (36) we used Eqs. (12) and (32) and assumed C = 1 mb/Sr. For comparison we have also plotted the corresponding electro-Primakoff cross-section (solid curves) on the diagrams.

We next consider the bremsstrahlung radiation problem. Here one can take advantage of the highly peaked nature of the bremsstrahlung radiation in minimizing this

background. We know that for very high energy electrons most of the bremsstrahlung radiation is emitted into small angles in the forward direction and the momentum transfer to the coulomb field is very small. Using an exponentially decreasing atomic potential Bethe[15] has shown that for small angles

$$\frac{d\sigma}{d\theta_k} = B\frac{\theta_k}{(\theta_o^2+\theta_k^2)^2}\left[\log\frac{\theta_o^2+\theta_k^2}{\theta_o^2} + D\right] \qquad (37)$$

where $\theta_o = m_e/E_i$ and B and D are independent of θ_k, the angle made by the bremsstrahlung photon with respect to the incident electron beam. Since the logarithm term in (37) varies rather slowly, the angular dependence of the bremsstrahlung cross-section is essentially given (for small angles) by the factor $\theta_k/(\theta_o^2+\theta_k^2)^2$. The maximum[16] then occurs at $\theta_o/\sqrt{3}$, and the cross-section falls off steeply with increase in θ_k. We note that for 10 Gev electrons $\theta_o \simeq 5\times10^{-5}$ and at $\theta_k = 5\times10^{-4}$, the cross-section is already down by a factor of $\sim10^{-3}$. The π° production cross-section by the bremsstrahlung photons (via Primakoff and nuclear processes) will thus be essentially symmetrical around the forward direction and would exhibit a sharp peak (Primakoff peak) at an angle $\theta_\pi = \theta_P = m_\pi^2/2E_\pi^2$, and a wider peak (coherent nuclear production peak) at $\theta_\pi = \theta_c \simeq \frac{1}{\sqrt{6}\cdot E_\pi}$. (Here θ_π denotes the π° production angle with respect to the incident electron beam). Now the angular distribution of the π° produced in the electro-Primakoff

process will be also highly peaked, but it should be noticed that, unlike the π^os produced by the bremsstrahlung photons, the symmetry axis of the electro-Primakoff pions will be around the direction θ_k of the exchanged virtual photon and not around the forward direction. Thus, if the kinematics of the apparatus is so arranged that $\theta_k >> \theta_c$, the electro-Primakoff peak will occur in a region where the bremsstrahlung background will be small. The condition $\theta_k >> \theta_c$ can be met by making the final electron to scatter at an angle $\theta_e \cong \frac{E_\pi}{E_f}\theta_k >> \frac{1}{\sqrt{b}E_f}$, or, equivalently by having $-k^2 >> E_i/(bE_f)$. In the energy region of our interest this condition can be satisfied.

References

1. H. Primakoff, Phys. Rev. 181, 899 (1951).
2. V. Glaser and R.A. Ferrell, Phys. Rev. 121, 886 (1961).
3. C. Chiuderi and G. Morpurgo, Nuovo Cimento 19, 497 (1961).
4. C.A. Engelbrecht, Phys. Rev. 133B, 988, (1964).
5. G. Morpurgo, Nuovo Cimento 31, 569 (1964).
6. G. Bellettini, C. Bemporado, P.I. Braccini and L. Foà, Nuovo Cimento 90A, 1139 (1965).
7. B. Margolisk Phys. Letters 26B, 524 (1968); Nuclear Physics B6, 85 (1968).
8. G. Bellettini, C. Bemporad, P.L. Braccini, C. Bradaschia, L. Foà, K. Lübelsmeyer and D. Schmitz, Nuovo Cimento 56A, 243 (1970).
9. J.D. Bjorken and S.D. Drell, Relativistic Quantum Mechanics, McGraw Hill Book Company, New York (1965).
10. C.F. Weizsäcker, Z. Physik 88, 612 (1934); E.J. Williams, Kgl. Danske Videnskab. Selskab, Mat.-fys. Medd. 13, No. 4 (1935).
11. R.B. Curtis, Phys. Rev. 104, 211 (1956). For a more exhaustive reference on this technique, see S.J. Brodsky, T. Kinoshita and H. Terazawa, Phys. Rev. 4D, 1532 (1971).
12. B.E. Lautrup and J. Smith, Phys. Rev. D3, 1122 (1971) and other earlier references contained in this paper.
13. N.P. Samios, Phys. Rev. 121, 275 (1961), H. Kobrak, Nuovo Cimento 20, 1115 (1961).

14. S. Devons et. al., Phys. Rev. 184, 1356 (1969).

15. H. Bethe, Proc. Camb. Phil. Soc. 30, 524 (1934).

16. M. Stearns (Phys. Rev. 76, 836 (1949)) has worked out the root mean square angle of emission of photons in radiation processes of electrons. His result may be written as $\sqrt{<\theta^2>} = f(E_i,E_f,Z) \frac{m_e}{E_i} \ln(E_i/m_e)$, where $f(E_i,E_f,Z)$ is less than 1.

Weizsäcker-Williams Approximation

In analogy to the Primakoff process let us consider a photoproduction reaction $\gamma + z \rightarrow z' + X$ where a particle X is produced by a nucleus z. The amplitude for this process can be written as

$$A = \epsilon_\mu(k,\lambda) m_\mu \tag{A1}$$

where $\epsilon_\mu(k,\lambda)$ is the polarization vector of the photon with polarization λ and four-momentum k. For the real photon case $k^2 = 0$ and gauge condition requires that

$$k_\mu m_\mu = 0 \tag{A2}$$

The differential cross section is given by

$$\frac{d\sigma}{d\Omega_x} = \frac{1}{32\pi^2} \frac{|\vec{p}_x|}{E_x} |\vec{m}|^2 \tag{A3}$$

where we have averaged over the photon polarizations and neglected the recoil energy of the nucleus.

The amplitude for the corresponding electro-production process can be written as

$$B = \frac{e}{k^2}[\bar{u}(p_f,s_f)\gamma_\mu\ u(p_i,s_i)]M_\mu, \tag{A4}$$

where we have used the conventional notations for the spinors. The conservation of electromagnetic current requires that

$$k_\mu M_\mu = (p_i - p_f)_\mu M_\mu = 0 \tag{A5}$$

We can thus replace M_o by $\vec{k}.\vec{M}/k_o$ and express M_μ in terms of $\vec{M}$ only. To calculate the cross-section, we average over the initial electron spin states and sum over all final spin states. Then

$$\frac{1}{2}\Sigma|B|^2 = \frac{1}{4m_e^2}\left[|k^2|M^2 + 4(p_i.M)^2\right] \tag{A6}$$

where we have used the fact that $p_i.M = p_f.M$. For the real photon, the matrix element has only a transverse component, i.e., $\vec{k}.\vec{m} = 0$, but for the virtual photon there is a longitudinal component as well. Let us write

$$\vec{M} = \vec{M}_T + \vec{M}_L \tag{A7}$$

where $\vec{k}.\vec{M} = \vec{k}.\vec{M}_L$ and $\vec{k} \times \vec{M}_L = 0$. Note that as $k^2 \to 0$, $\vec{M}_T \to \vec{m}$, $\vec{M}_L \to 0$ and therefore $M_\mu \to m_\mu$.

We shall now describe the Weizsacker-Williams (W-W) approximation method, which was invented to obtain roughly the results of collisions induced by charged particles from a knowledge of the corresponding photon-induced reactions. This technique is applicable only for the case of a relativistic charged particle undergoing a very small deflection. We first note[11] that when the electron scattering angle is very small, one can approximate the contribution of $|\vec{p}_i.\vec{M}_T|^2$ in terms of $|\vec{M}_T|^2$ in the following way

$$\lim_{\theta_e \to 0} \int_0^{2\pi} |\vec{p}_i.\vec{M}_T|^2 d\varphi_e = \lim_{\theta_e \to 0} \frac{\vec{p}_i^{\,2}\vec{p}_f^{\,2}}{2\vec{k}^2} \sin^2\theta_e \int_0^{2\pi} |\vec{M}_T|^2 d\varphi_e \tag{A8}$$

Thus if we are interested in the cross-section integrated over the outgoing azimuthal angle we can approximately replace

$$|\vec{p}_i.\vec{M}_T|^2 \xrightarrow[\theta_e \to 0]{} \frac{\vec{p}_i^{\,2}\vec{p}_f^{\,2}}{2\vec{k}^2} \sin^2\theta_e |\vec{M}_T|^2 \tag{A9}$$

In the W-W approximation one neglects the M_L terms compared to the M_T terms and uses equation (A9) to write the whole

cross-section in terms of $|\vec{M}_T|^2$. One then obtains the following expression for the electro-production cross-section

$$\frac{d^3\sigma}{dE_f d\Omega_f d\Omega_x} = \frac{e^2}{(2\pi)^5} \frac{|\vec{p}_x||\vec{p}_f||\vec{M}_T|^2}{8v_i E_i k^4} \left\{ |k^2| + \frac{2\vec{p}_i^{\,2}\vec{p}_f^{\,2}}{\vec{k}^2} \sin^2\theta_e + \ldots \right\} \tag{A10}$$

In the same spirit of approximation, one now replaces $|\vec{M}_T|^2$ by the real photon cross-section given in Eq. (A3) and finally obtains the desired expression:

$$\left(\frac{d^3\sigma}{dE_f d\Omega_f d\Omega_x}\right)_{\text{electro}} = \frac{\alpha}{2\pi^2} \frac{E_f E_x}{v_i E_i k^4} \left[|k^2| + \frac{2E_i^2 E_f^2}{\vec{k}^2} \sin^2\theta_e + \ldots \right] \left(\frac{d\sigma}{d\Omega_x}\right)_{\text{Photo}} \tag{A11}$$

We should now point out that in the electro-Primakoff process the longitudinal part of the amplitude identically vanishes, which makes this approximation procedure more justifiable. However, to obtain the electro-Primakoff results one still has to use Eq. (A9) and replace $\vec{M}_T$ by the amplitude for the Primakoff process.

Figure Captions

Fig. 1. Diagram showing the kinematics of the electro-Primakoff process.

Fig. 2. The co-ordinate system used in studying the electro-Primakoff effect. The outgoing pion makes an angle $(\theta_{\gamma\pi}, \phi_{\gamma\pi})$ with respect to this system, where the Z-axis is taken along the virtual photon momentum k and Y-axis is perpendicular to the plane defined by $\vec{p}_i$, $\vec{p}_f$ and $\vec{k}$.

Fig. 3. The shape of $\frac{d\sigma^{EP}}{d(\cos\theta_{\gamma\pi})}$ (arbitrary units) as a function of $\theta_{\gamma\pi}/\theta_E$ when $F_{e.m.}(\vec{q}^2) = 1$ and k^2, E_i, E_f and $\phi_{\gamma\pi}$ are kept fixed.

Fig. 4. The cross-section $Z^{-2}\frac{d\sigma^{EP}}{d(\cos\theta_{\gamma\pi})}$ given by Eq. (29) is plotted as a function of $\theta_{\gamma\pi}/\theta_E$ for E_i = 10 Gev and $\langle|k^2|\rangle = 0.5$ (Gev/c)^2. To display the effect of electromagnetic form factor on the differential cross-section, three values of b, namely, 0, 10 and 300 (Gev/c)$^{-2}$ are used. Fig. 4a is for $\langle E_f\rangle$ = 4 Gev and Fig. 4b for $\langle E_f\rangle$ = 8 Gev.

Fig. 5. Plot of $Z^{-2}\Delta\sigma^{EP}$ given by Eq. (31) as a function of $\langle|k^2|\rangle$ for different values of b. E_i = 10 Gev for all the curves. The solid (dashed) curves are for $\langle E_f\rangle$ = 4 Gev (8 Gev). For details see text.

Fig. 6. The effect of the form factor on the position of the electro-Primakoff peak. $\theta_E = \frac{-k^2 + m_\pi^2}{2E_\pi^2}$ gives the value of $\theta_{\gamma\pi}$ at which the electro-Primakoff peak occurs when the form factor effect is neglected, while $\bar{\theta}_E$ gives the corresponding value when the form factor effect is included in the theory.

Fig. 7. The differential cross-sections for the coherent nuclear background (dashed curves) and electro-Primakoff effect (solid curves) are plotted against $\theta_{\gamma\pi}/\theta_E$ for hydrogen ($b = 10$ $(\text{Gev}/c)^{-2}$) and lead ($b = 300$ $(\text{Gev}/c)^{-2}$) targets and for various values of k^2 and E_π. E_π is 6 Gev in Figs. 7a - 7c and 2 Gev in Figs. 7d and 7e. The values of $|k^2|$ are indicated in the diagrams. The solid curves in Fig. 7c are the same as the corresponding curves in Fig. 4b.

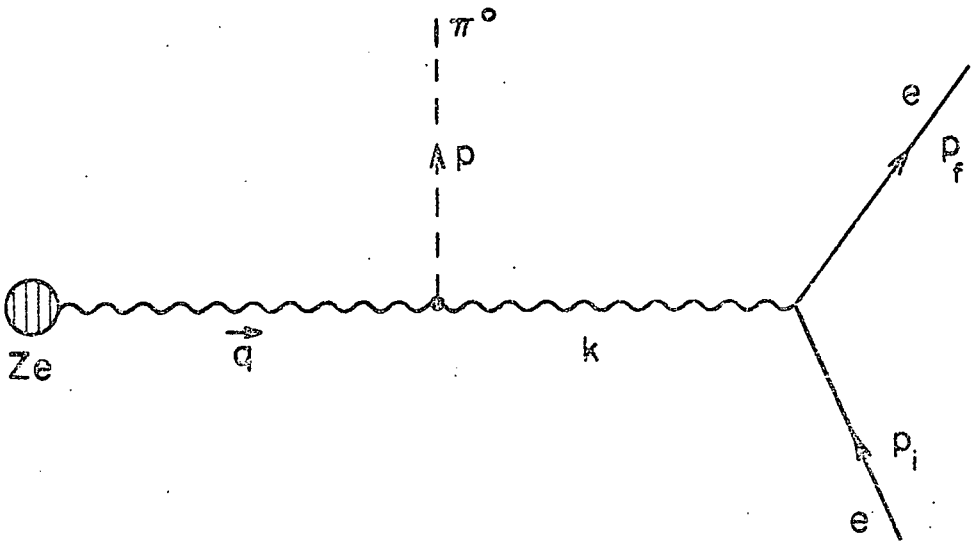

Fig. 1

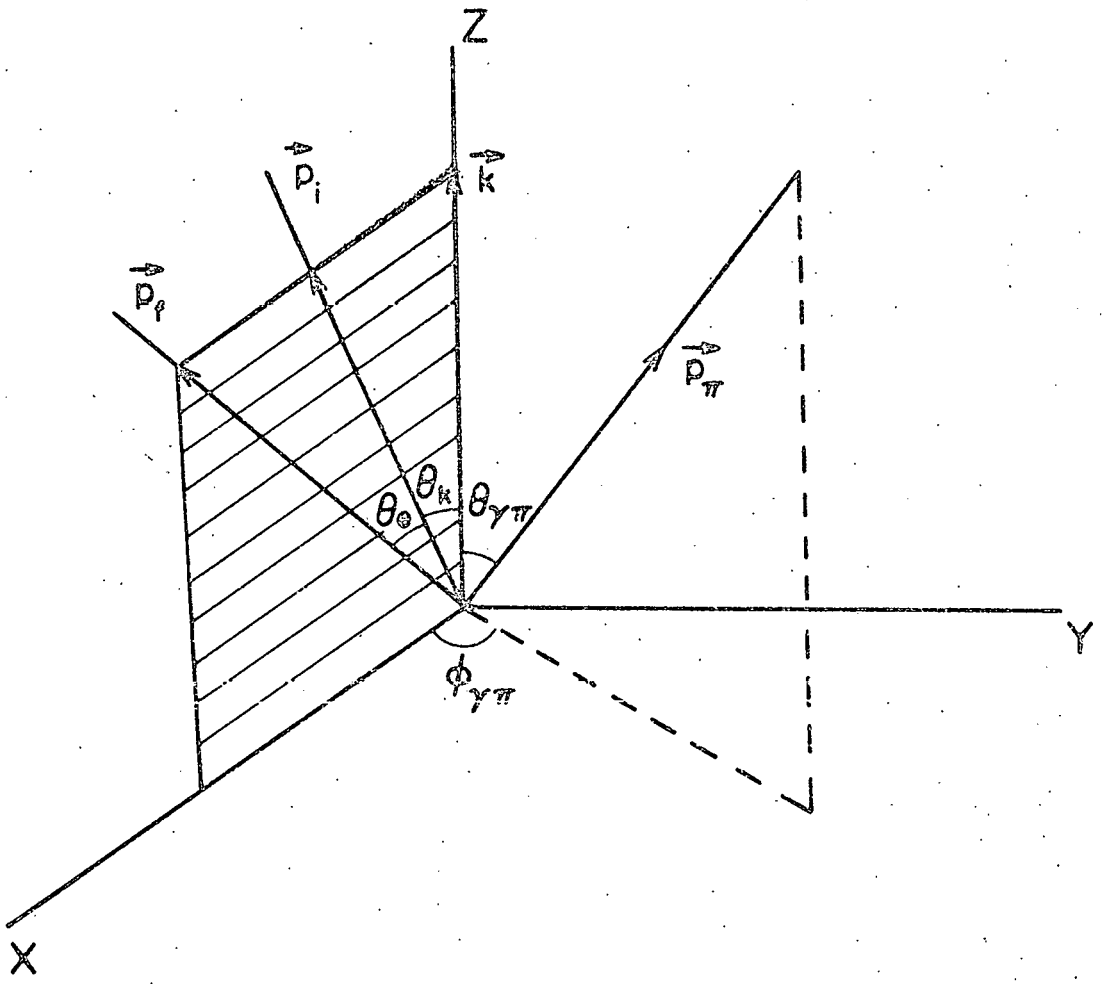
Z
$\vec{p}_i$
$\vec{k}$
$\vec{p}_f$
$\vec{p}_\pi$
θ_e
θ_k
$\theta_{\gamma\pi}$
$\phi_{\gamma\pi}$
Y
X

Fig. 2.

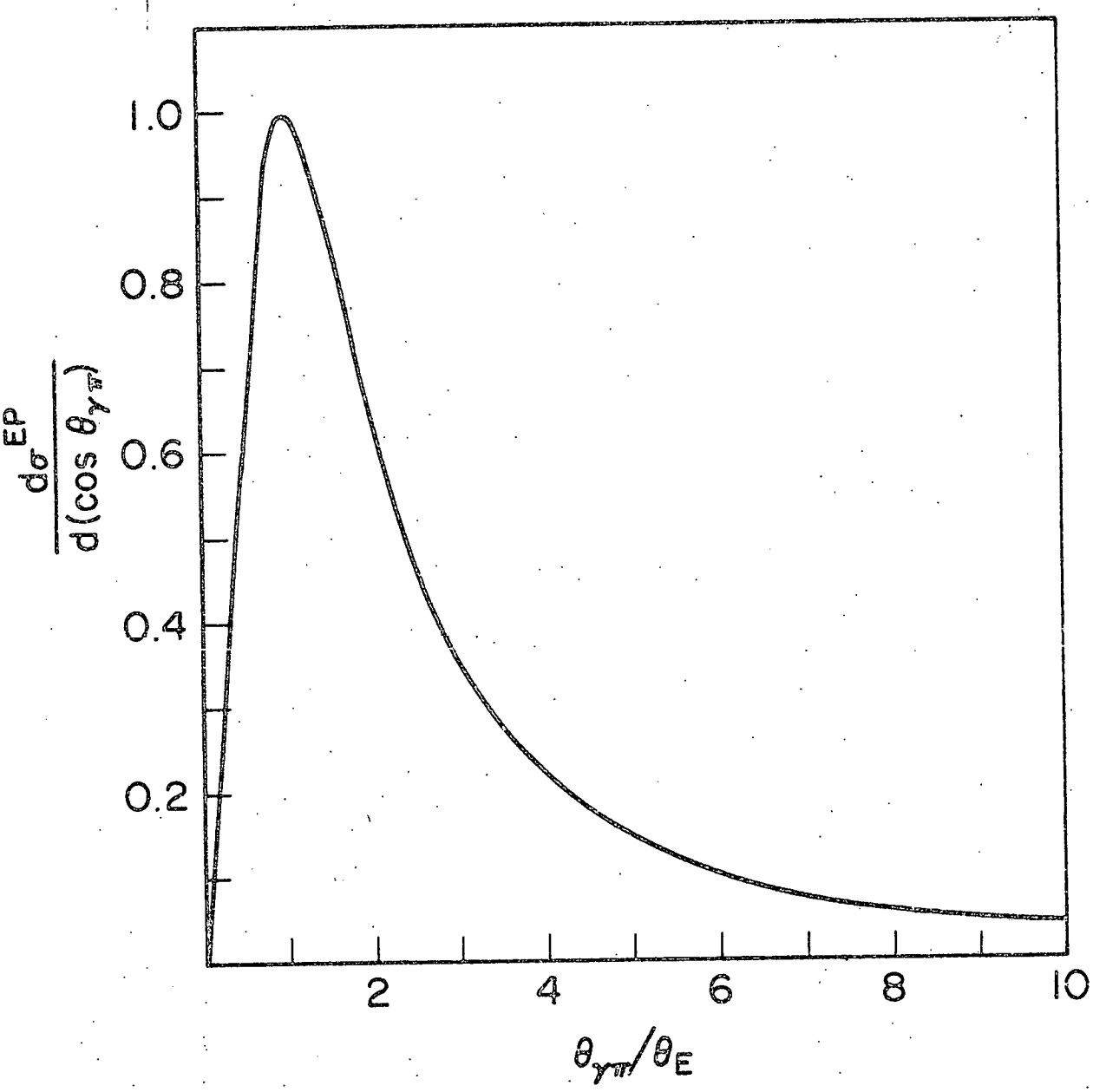
1.0
0.8
0.6
0.4
0.2
$\frac{d\sigma^{EP}}{d(\cos\theta_{\gamma\pi})}$
2
4
6
8
10
$\theta_{\gamma\pi}/\theta_E$

Fig. 3.

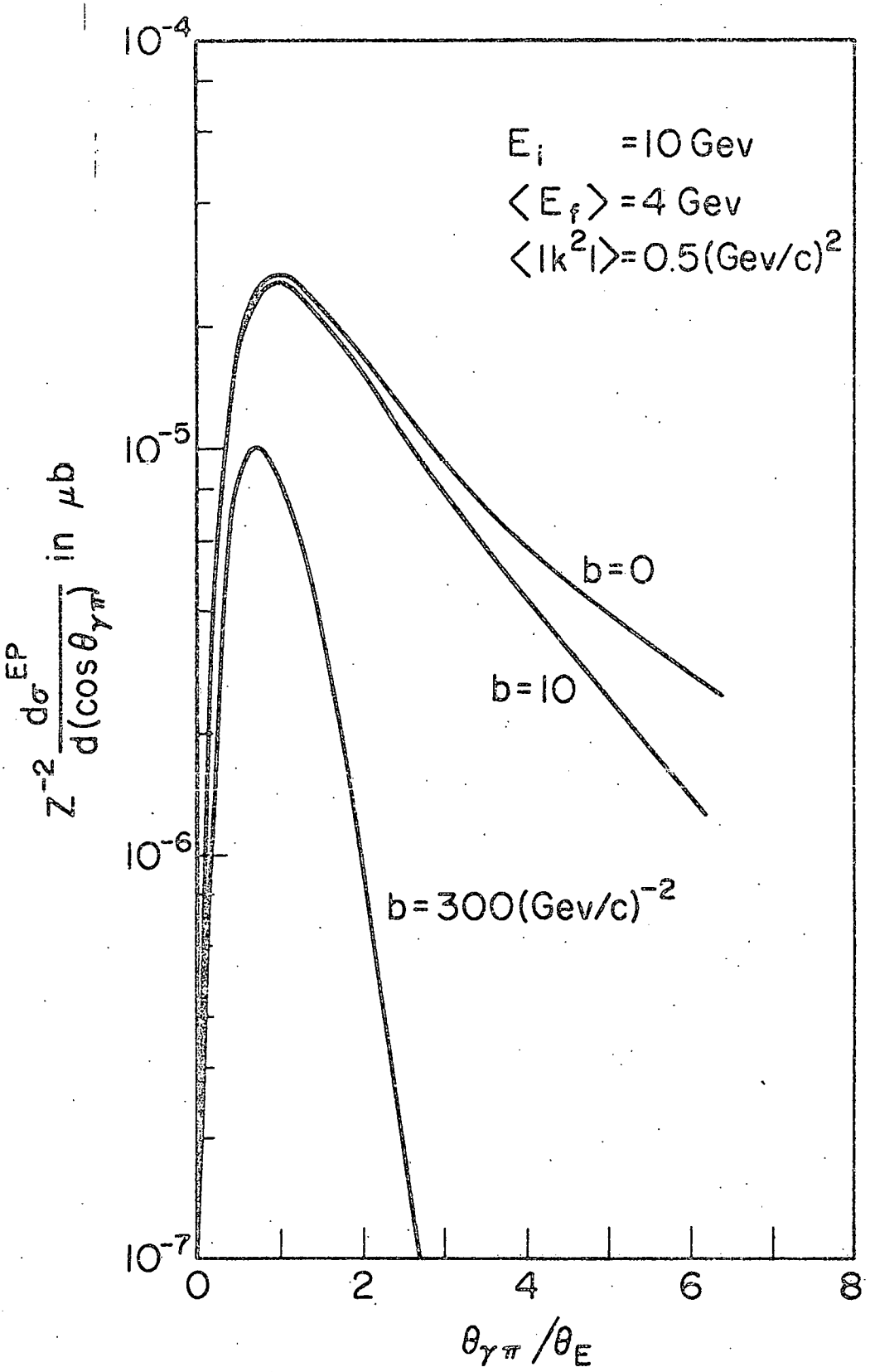
10^{-4}
10^{-5}
10^{-6}
10^{-7}
E_i = 10 Gev
$\langle E_f \rangle$ = 4 Gev
$\langle |k^2| \rangle$ = 0.5 (Gev/c)^2
b = 0
b = 10
b = 300 (Gev/c)$^{-2}$
$Z^{-2} \frac{d\sigma^{EP}}{d(\cos\theta_{\gamma\pi})}$ in μb
0
2
4
6
8
$\theta_{\gamma\pi}/\theta_E$

Fig. 4a.

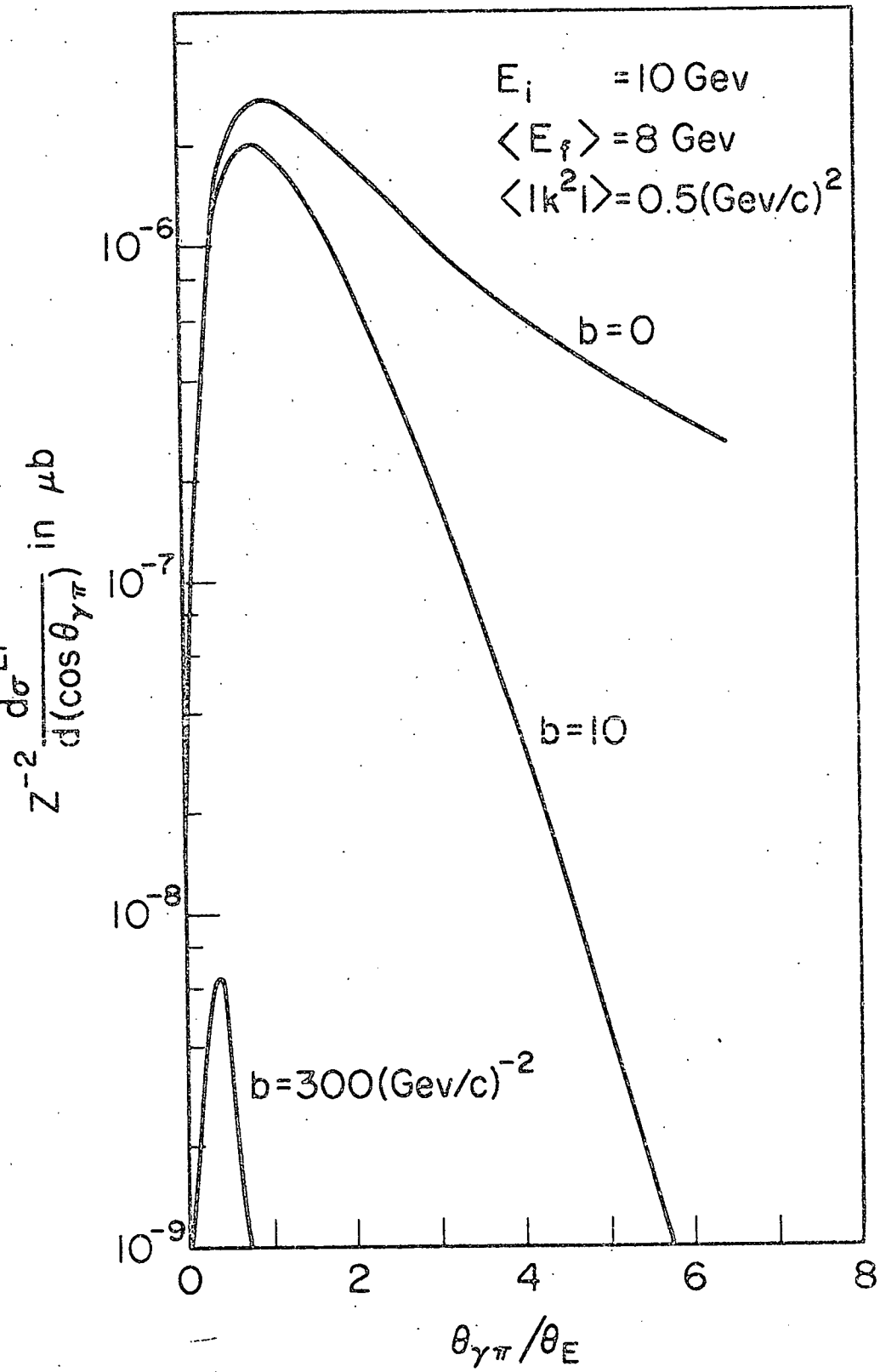
E_i = 10 Gev
$\langle E_f \rangle$ = 8 Gev
$\langle |k^2| \rangle$ = 0.5(Gev/c)^2
b = 0
b = 10
b = 300(Gev/c)$^{-2}$
10^{-6}
10^{-7}
10^{-8}
10^{-9}
0
2
4
6
8
$Z^{-2} \frac{d\sigma^{EP}}{d(\cos\theta_{\gamma\pi})}$ in μb
$\theta_{\gamma\pi}/\theta_E$

Fig. 4b.

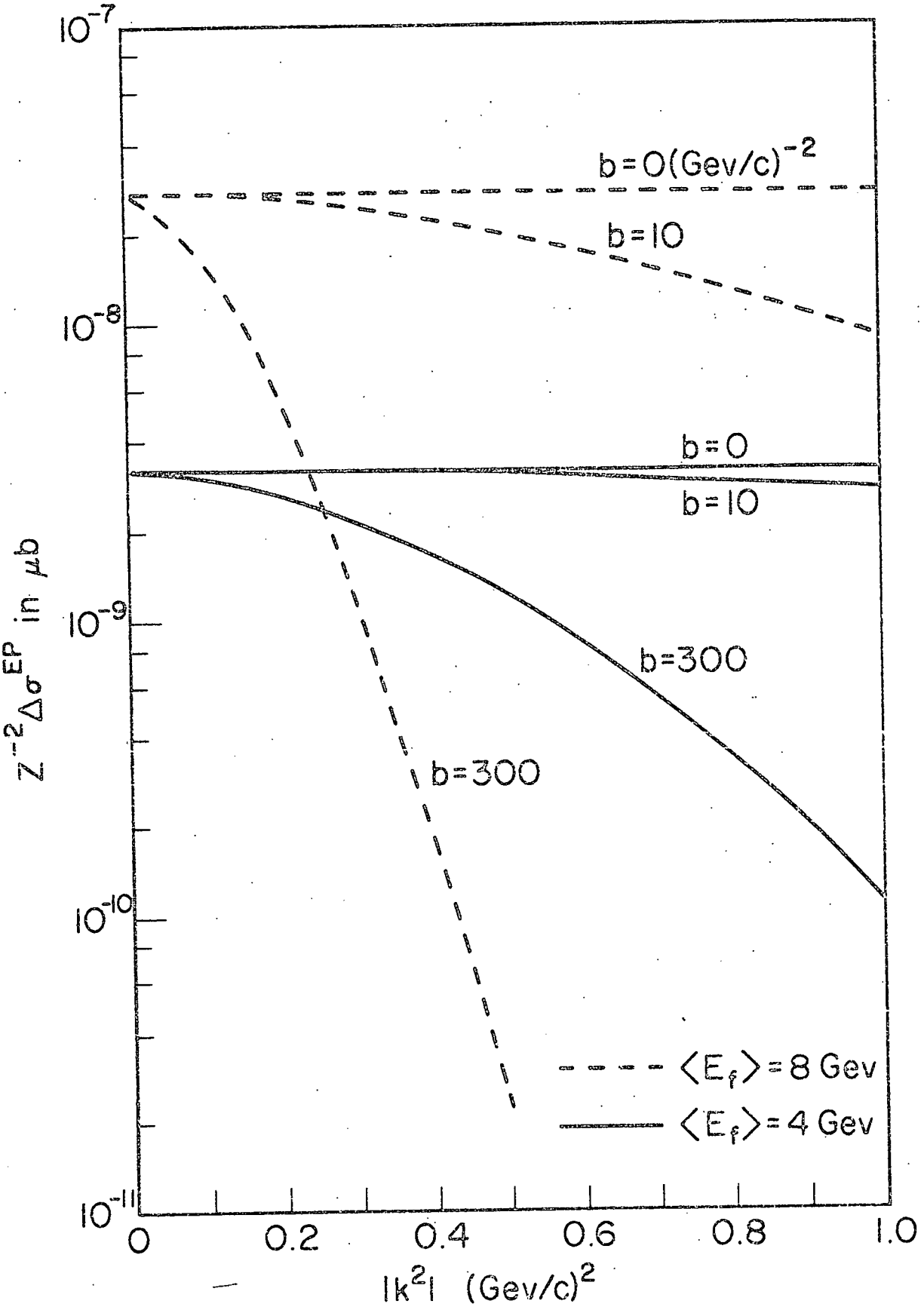
10^{-7}
10^{-8}
10^{-9}
10^{-10}
10^{-11}
$Z^{-2}\Delta\sigma^{EP}$ in μb
b=0(Gev/c)$^{-2}$
b=10
b=0
b=10
b=300
b=300
$\langle E_f \rangle$ = 8 Gev
$\langle E_f \rangle$ = 4 Gev
0
0.2
0.4
0.6
0.8
1.0
$|k^2|$ (Gev/c)^2

Fig. 5.

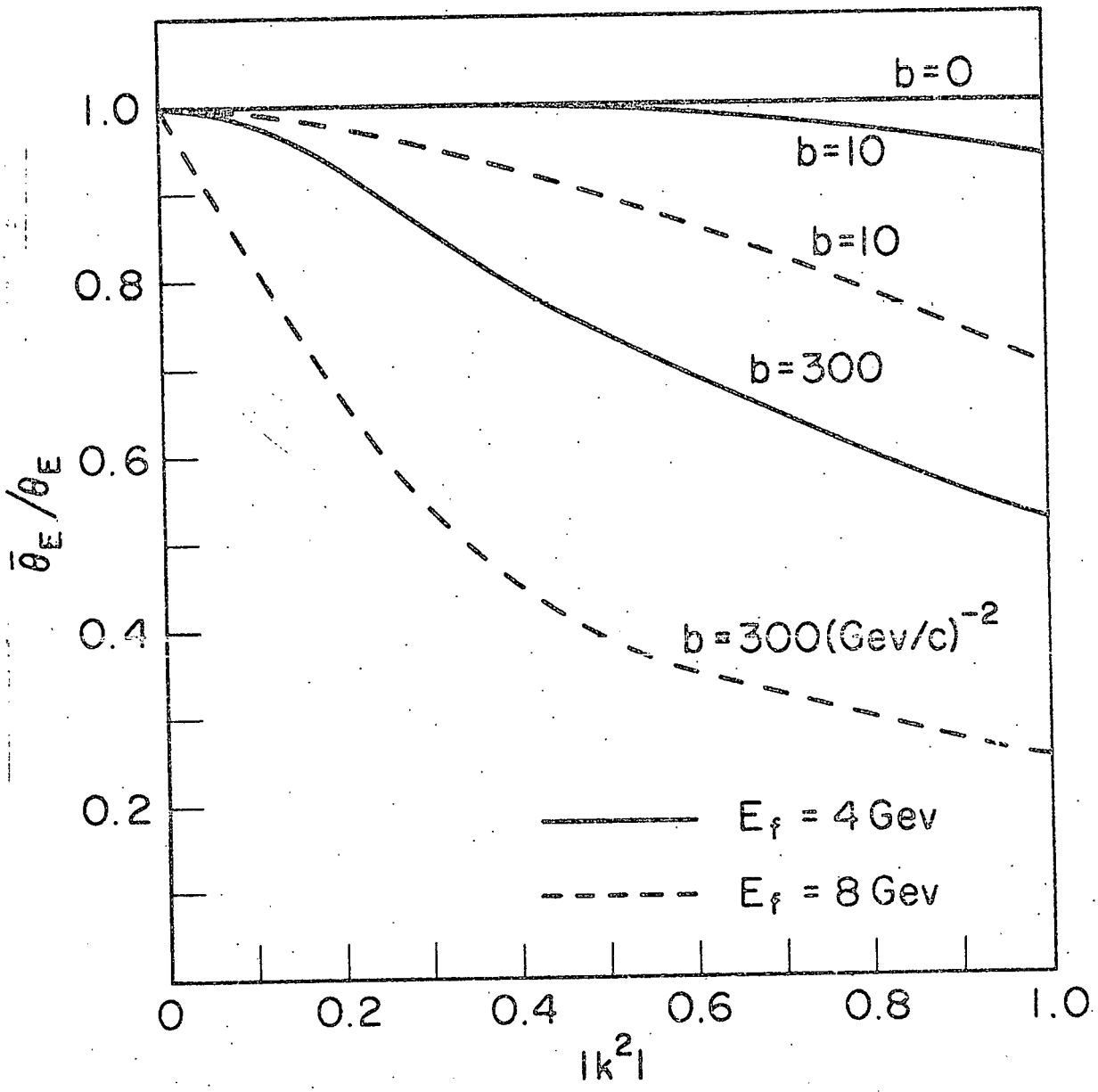
b=0
b=10
b=10
b=300
b=300(Gev/c)$^{-2}$
E_f = 4 Gev
E_f = 8 Gev
$\bar{\theta}_E/\theta_E$
$|k^2|$
1.0
0.8
0.6
0.4
0.2
0
0.2
0.4
0.6
0.8
1.0

Fig. 6.

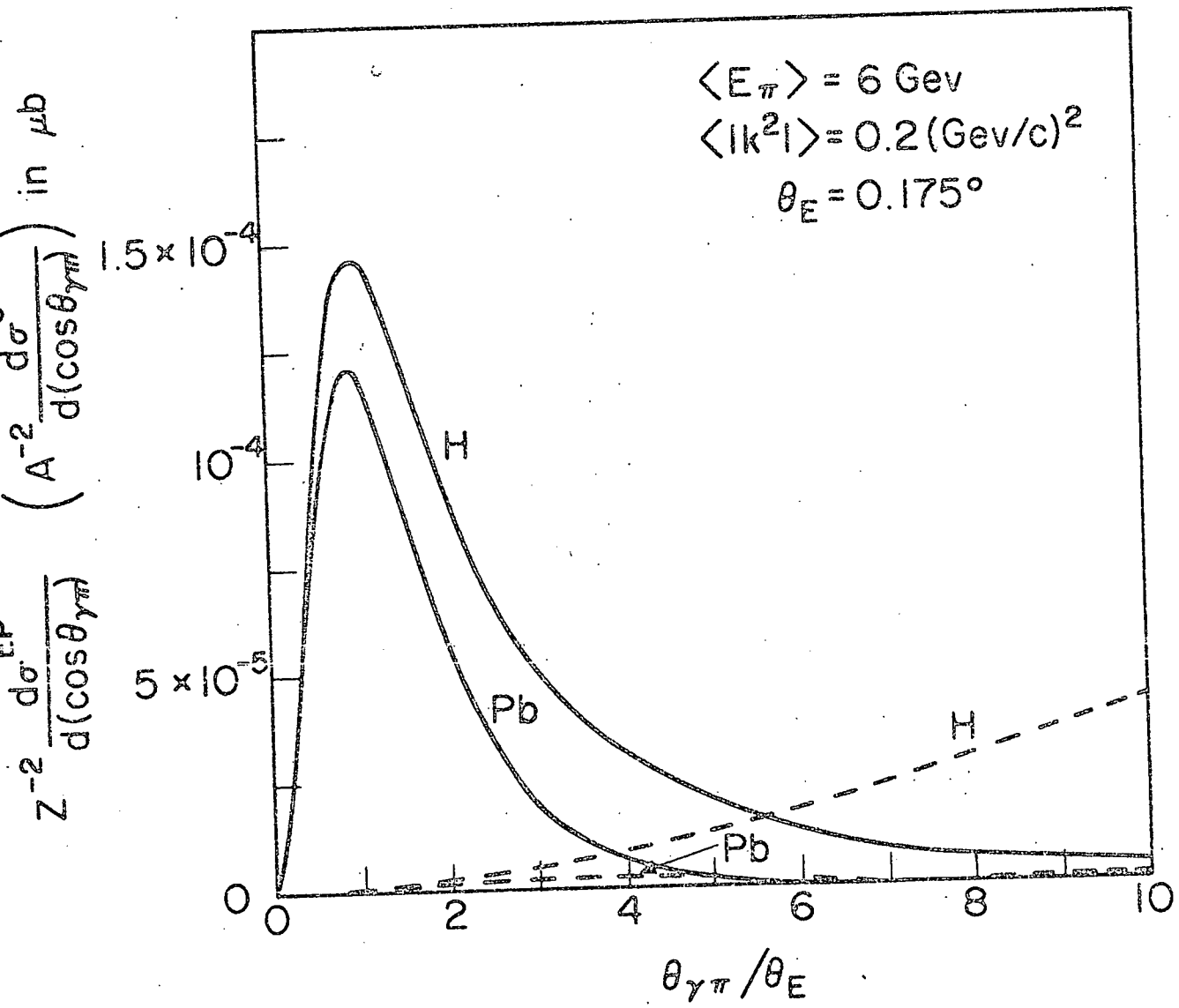
$\langle E_\pi \rangle$ = 6 Gev
$\langle |k^2| \rangle$ = 0.2 (Gev/c)^2
θ_E = 0.175°
$Z^{-2} \frac{d\sigma^{EP}}{d(\cos\theta_{\gamma\pi})}$ $\left(A^{-2} \frac{d\sigma^{C}}{d(\cos\theta_{\gamma\pi})} \right)$ in μb
1.5×10^{-4}
10^{-4}
5×10^{-5}
0
H
Pb
H
Pb
0
2
4
6
8
10
$\theta_{\gamma\pi}/\theta_E$

Fig. 7a.

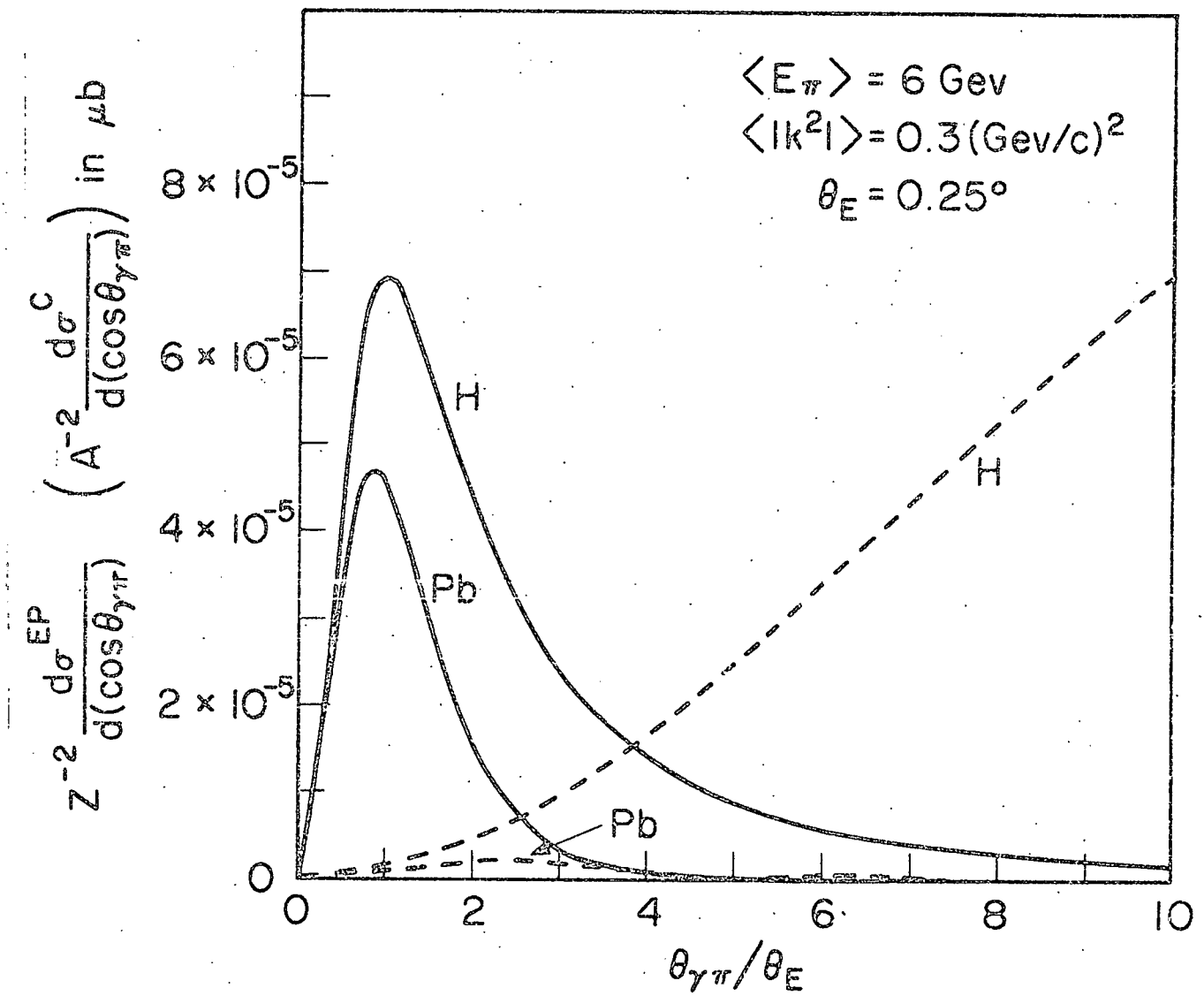
$\langle E_\pi \rangle$ = 6 Gev
$\langle |k^2| \rangle$ = 0.3 (Gev/c)^2
θ_E = 0.25°
$Z^{-2} \frac{d\sigma^{EP}}{d(\cos\theta_{\gamma\pi})}$ $\left(A^{-2} \frac{d\sigma^{C}}{d(\cos\theta_{\gamma\pi})}\right)$ in μb
8×10^{-5}
6×10^{-5}
4×10^{-5}
2×10^{-5}
0
H
Pb
H
Pb
0
2
4
6
8
10
$\theta_{\gamma\pi}/\theta_E$

Fig. 7b.

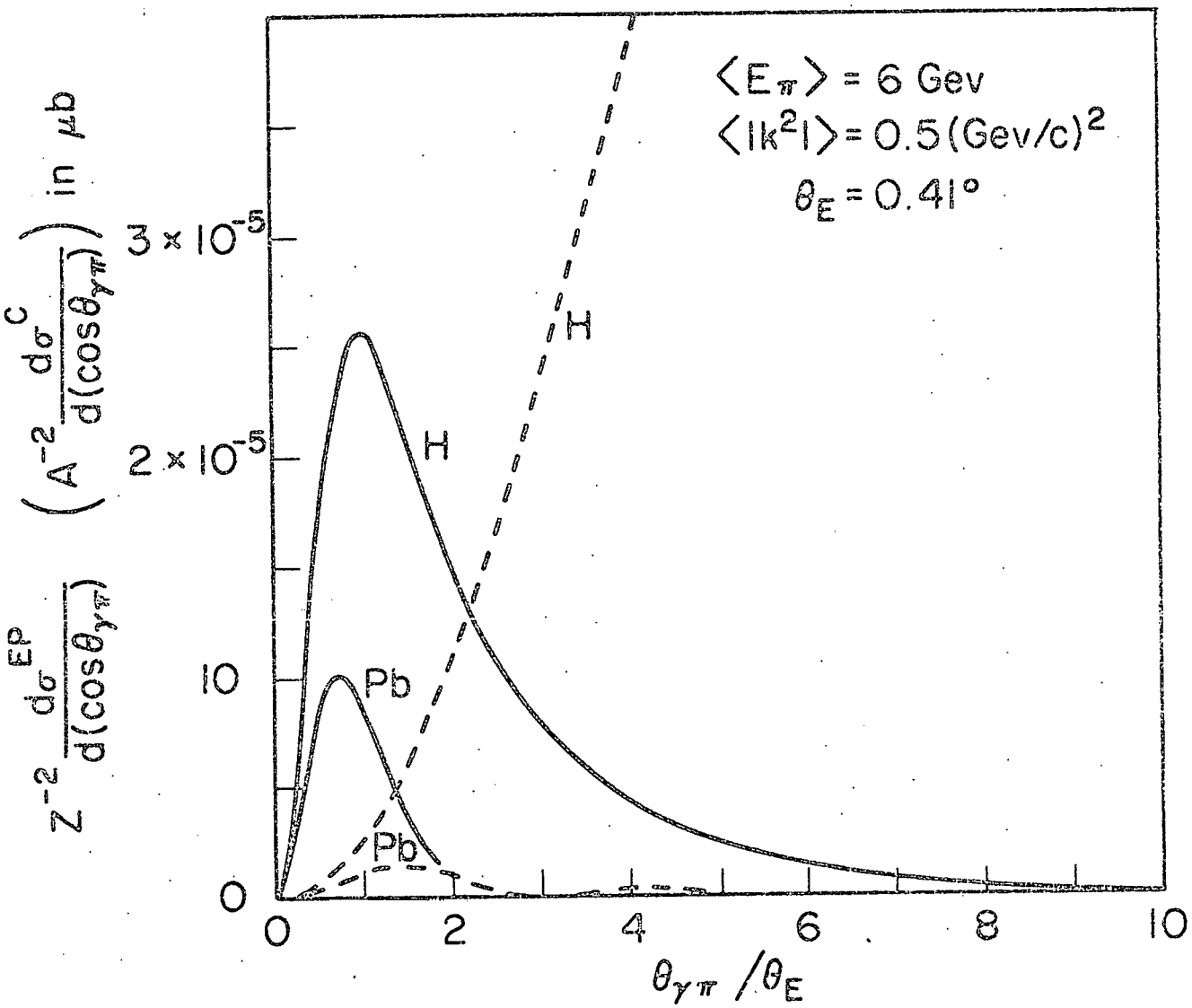
$\langle E_\pi \rangle$ = 6 Gev
$\langle |k^2| \rangle$ = 0.5 (Gev/c)^2
θ_E = 0.41°
H
H
Pb
Pb
$Z^{-2} \frac{d\sigma^{EP}}{d(\cos\theta_{\gamma\pi})} \left(A^{-2} \frac{d\sigma^{C}}{d(\cos\theta_{\gamma\pi})} \right)$ in μb
3 × 10^{-5}
2 × 10^{-5}
10
0
0
2
4
6
8
10
$\theta_{\gamma\pi} / \theta_E$

Fig. 7c.

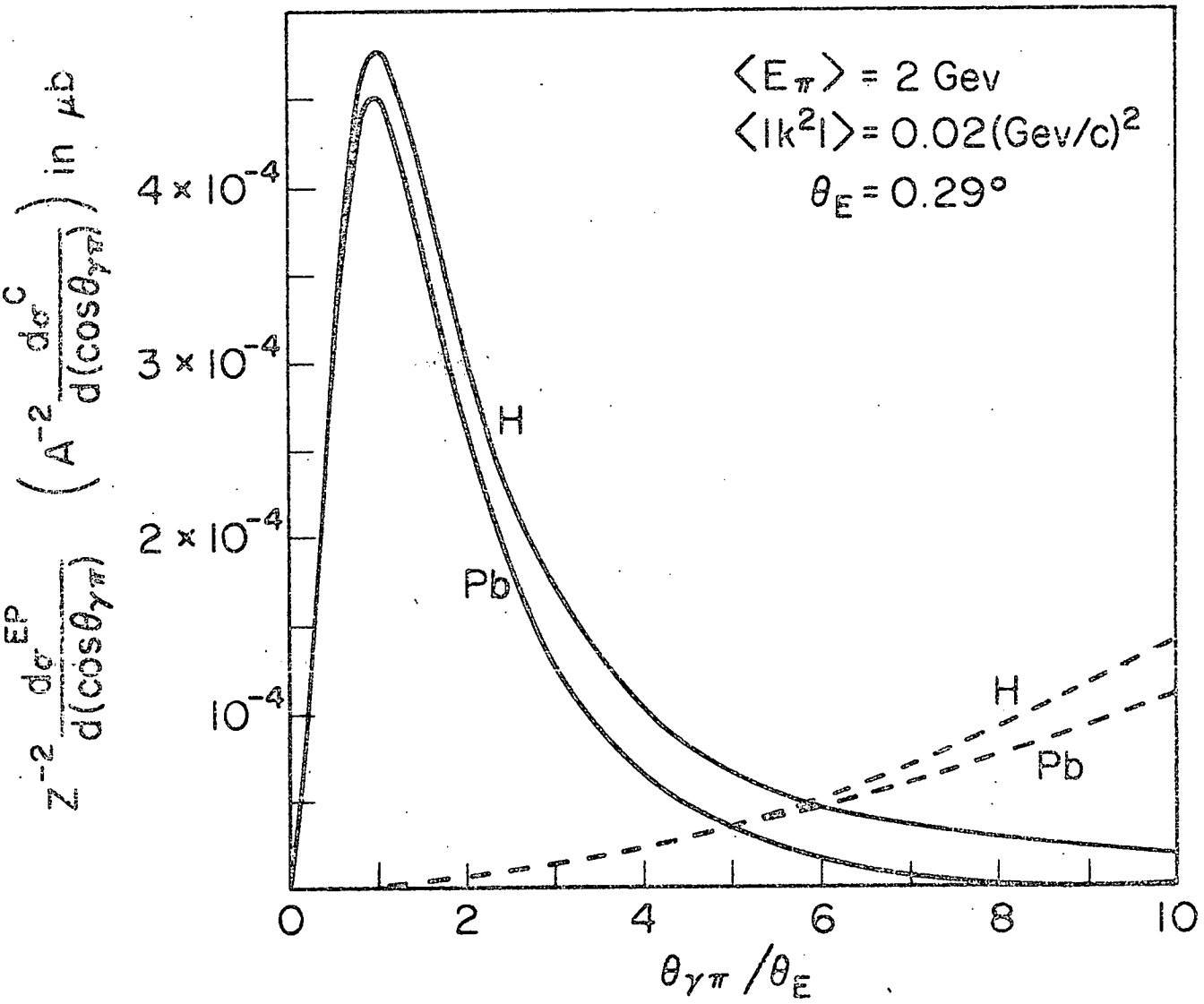
$\langle E_\pi \rangle$ = 2 Gev
$\langle |k^2| \rangle$ = 0.02(Gev/c)^2
θ_E = 0.29°
H
Pb
H
Pb
4×10^{-4}
3×10^{-4}
2×10^{-4}
10^{-4}
0
2
4
6
8
10
$\theta_{\gamma\pi}/\theta_E$
$Z^{-2} \frac{d\sigma^{EP}}{d(\cos\theta_{\gamma\pi})} \left(A^{-2} \frac{d\sigma^{C}}{d(\cos\theta_{\gamma\pi})} \right)$ in μb

Fig. 7d.

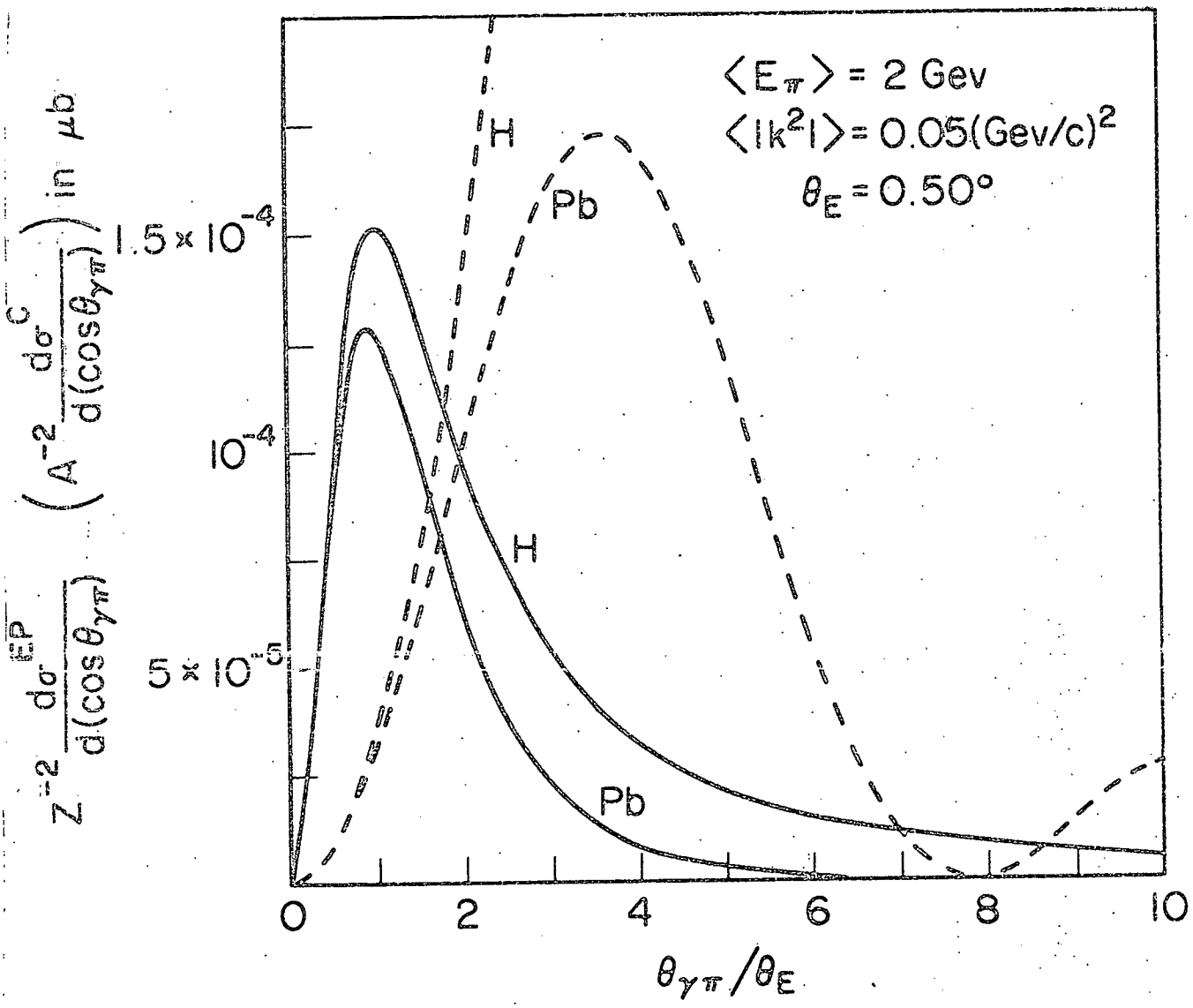
$\langle E_\pi \rangle$ = 2 Gev
$\langle |k^2| \rangle$ = 0.05(Gev/c)^2
θ_E = 0.50°
H
Pb
H
Pb
1.5×10^{-4}
10^{-4}
5×10^{-5}
$Z^{-2} \frac{d\sigma^{ep}}{d(\cos\theta_{\gamma\pi})}$ $\left(A^{-2} \frac{d\sigma^{c}}{d(\cos\theta_{\gamma\pi})}\right)$ in μb
0
2
4
6
8
10
$\theta_{\gamma\pi}/\theta_E$

Fig. 7e.